

Designing high performance polymer nanocomposites by incorporating robustness-controlled polymeric nanoparticles: insights from molecular dynamics

Guanyi Hou¹, Sai Li^{2,3}, Jun Liu^{2,3*}, Yunxuan Weng¹, Liqun Zhang^{2,3*}

1. College of Chemistry and Materials Engineering, Beijing Technology and Business University, People's Republic of China

2. State Key Laboratory of Organic-Inorganic Composites, Beijing University of Chemical Technology, People's Republic of China

3. Center of Advanced Elastomer Materials, Beijing University of Chemical Technology, People's Republic of China

Details of simulation model

In this study, both $\eta = 0$ and $\eta = 1.0$ were obtained same mean-square radius gyration, which was equal to approximately 5σ . The polymer matrix chains were fixed to be 100 beads, and each system contained 300 chains. For star-shaped nanoparticle (SSPNs), there are two sections: First section changed the hardness of NP, hence the η of star-shape systems were equal to 0.2, 0.4, 0.6, 0.8, respectively, and the arm length, L , was set as 10σ (Figure S1); Second section changed the arm length of star-shaped NP, hence L was equal to 5σ , 10σ , 15σ , 20σ , respectively, and η was set as 0.8. For all systems, the mass fraction of NPs was fixed as 20%. (Figure S2)

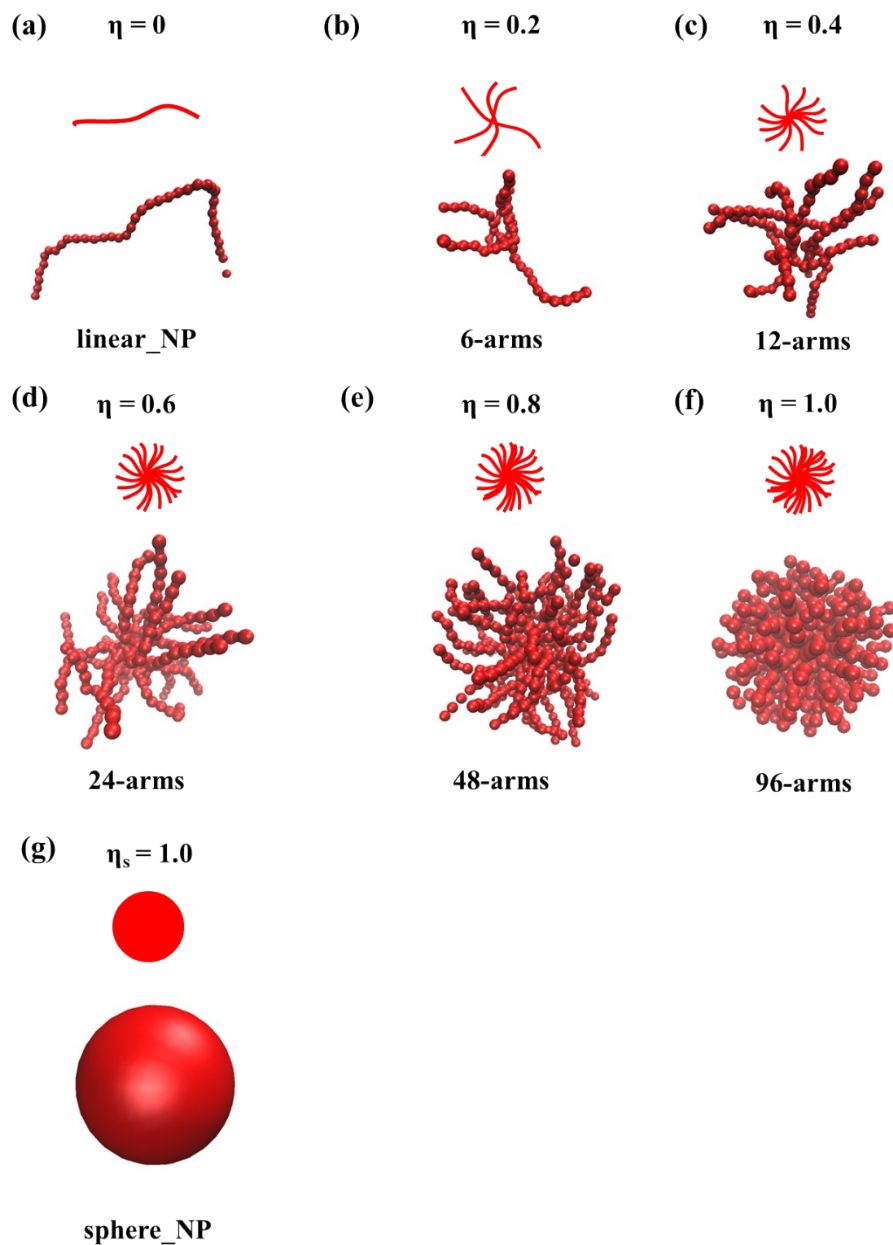


Figure S1. The schematic diagram of NP, including (a) $\eta = 0$; (b) $\eta = 0.2$; (c) $\eta = 0.4$; (d) $\eta = 0.6$; (e) $\eta = 0.8$; (f) $\eta = 1.0$; (g) $\eta_s = 1.0$; Noted that both linear NP and SSPNs were composed by the red-sphere bead that diameter was equal to 1σ .

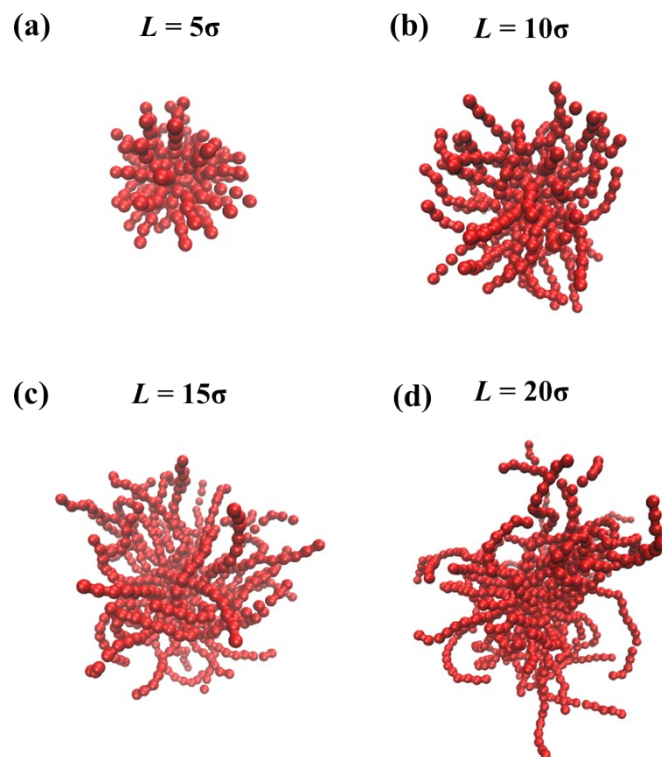


Figure S2. The schematic diagram for SSPNs with different L , where (a) $L = 5\sigma$; (b) $L = 10\sigma$; (c) $L = 15\sigma$; (d) $L = 20\sigma$. Noted that η was set as 0.8.

Table S1. the mean-root square radius of gyration (R_g) of NPs with different η .

system	R_g (σ)
$\eta = 0$	5.1108
$\eta = 0.2$	4.829
$\eta = 0.4$	4.94
$\eta = 0.6$	4.923
$\eta = 0.8$	4.78842
$\eta = 1.0$	4.9951
$\eta_s = 1.0$	5

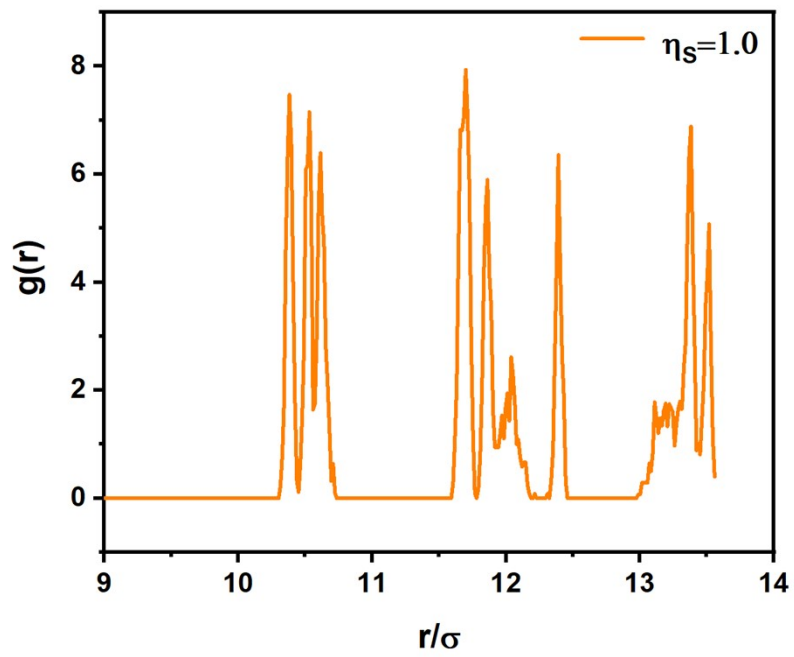


Figure S3. The radial distribution function of NP when $\eta_s = 1.0$.

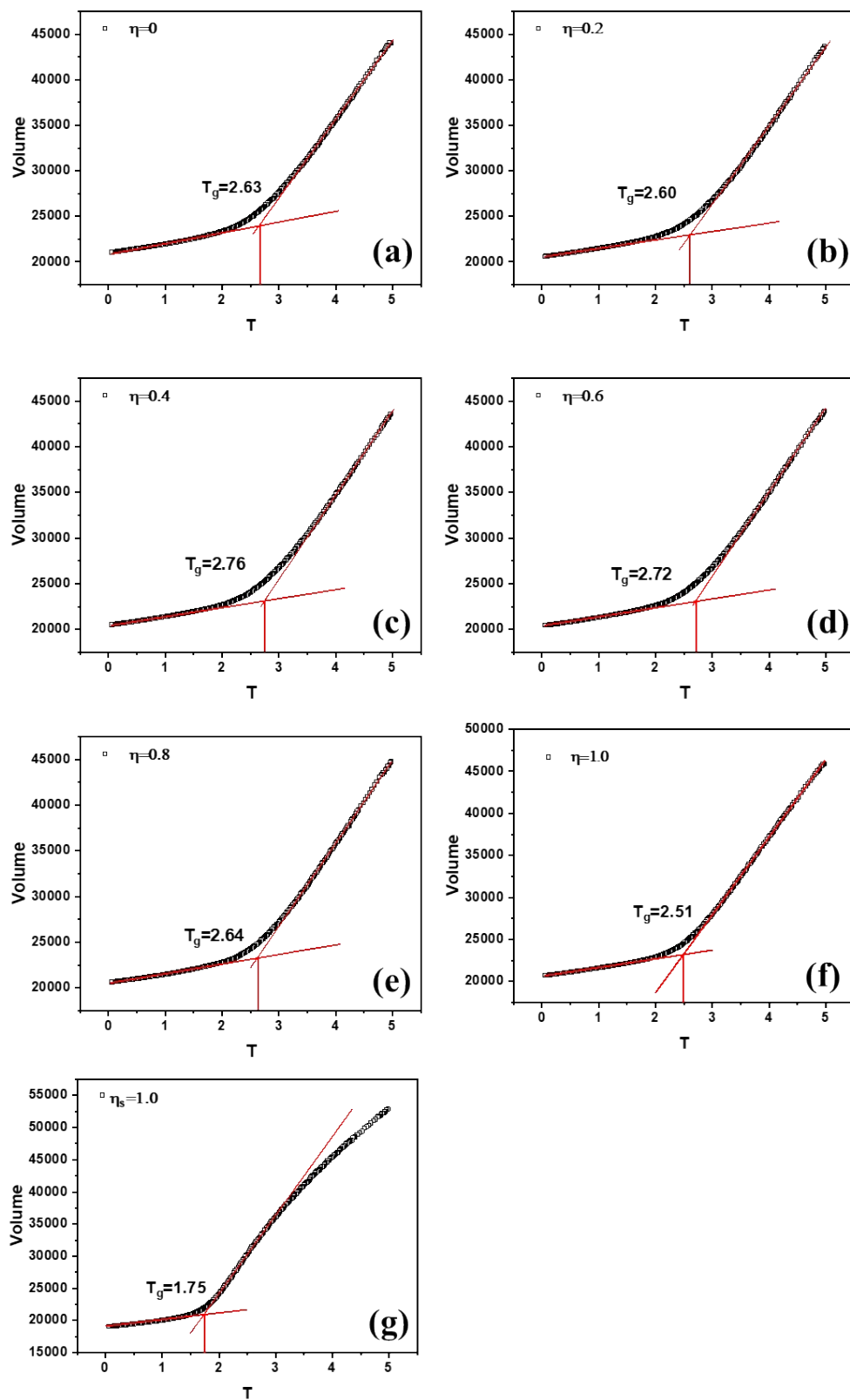
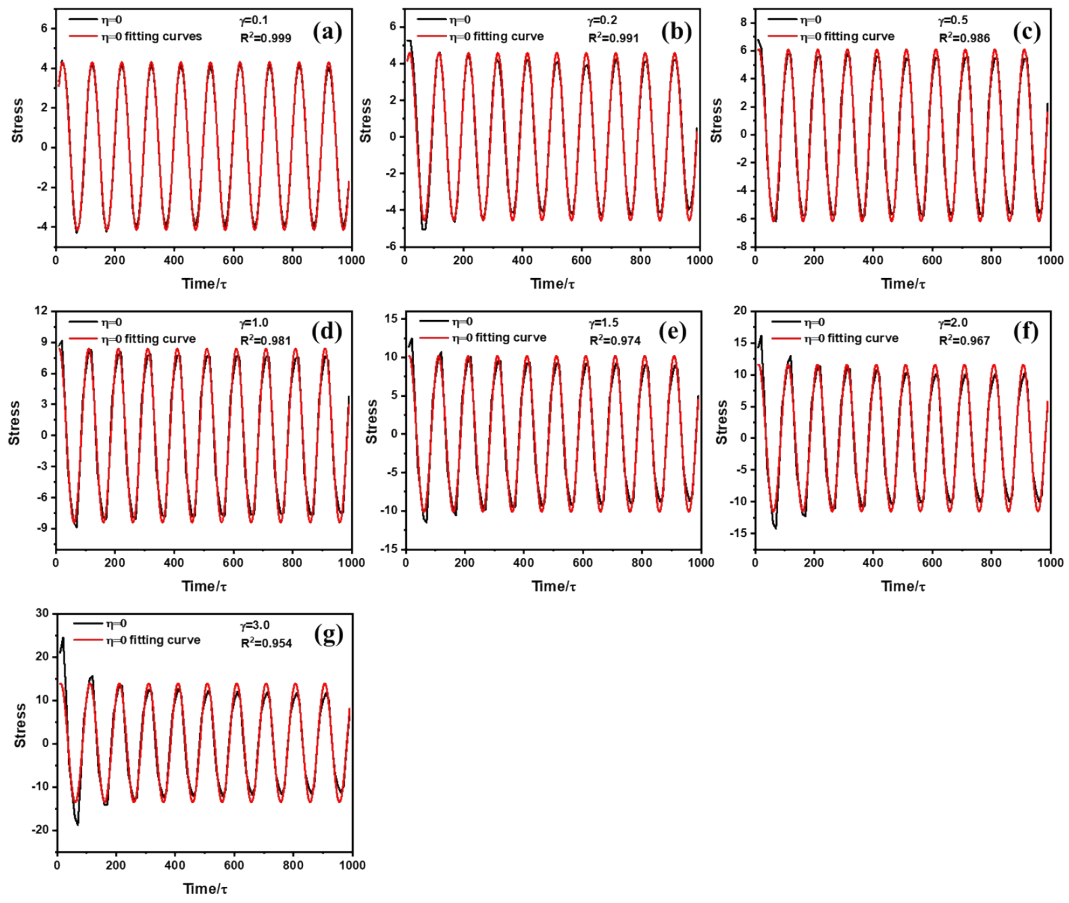
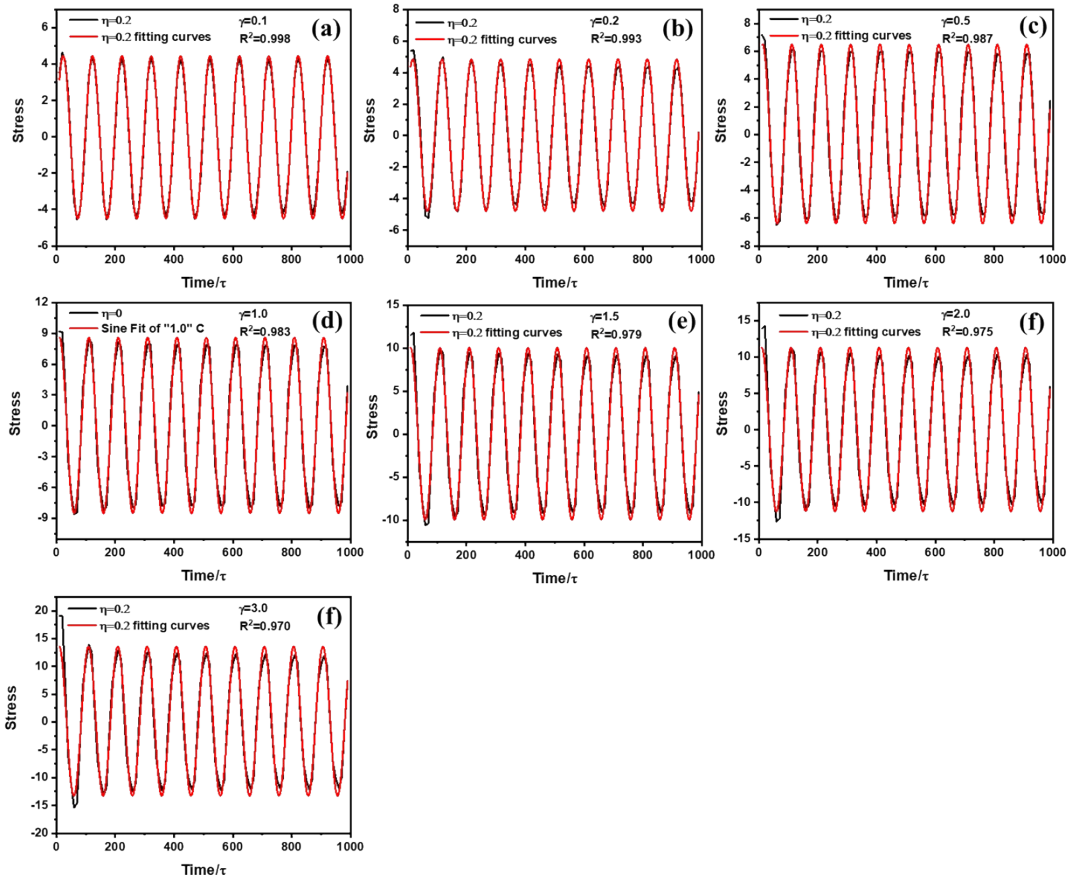


Figure S4. The glass transition temperature for PNCs when: (a) $\eta = 0$; (b) $\eta = 0.2$; (c) $\eta = 0.4$; (d) $\eta = 0.6$; (e) $\eta = 0.8$; (f) $\eta = 1.0$; (g) $\eta_s = 1.0$

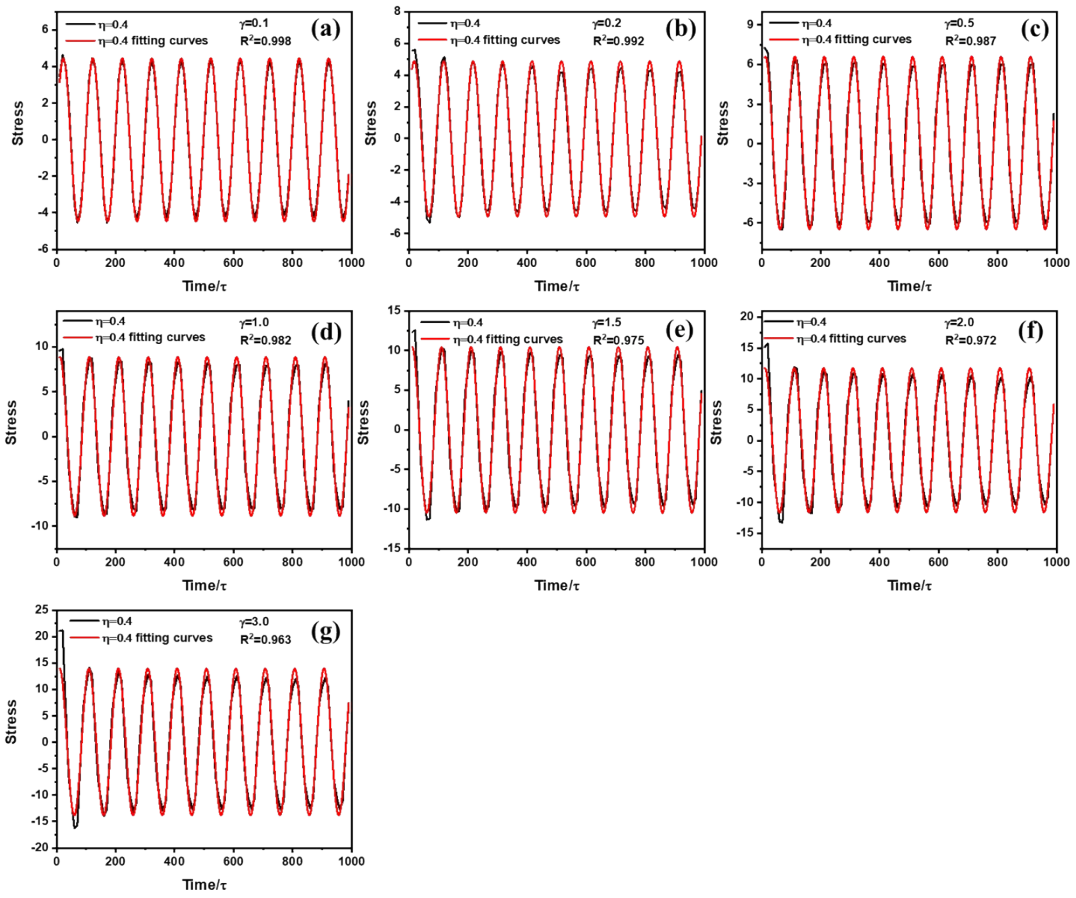
$\eta=0$



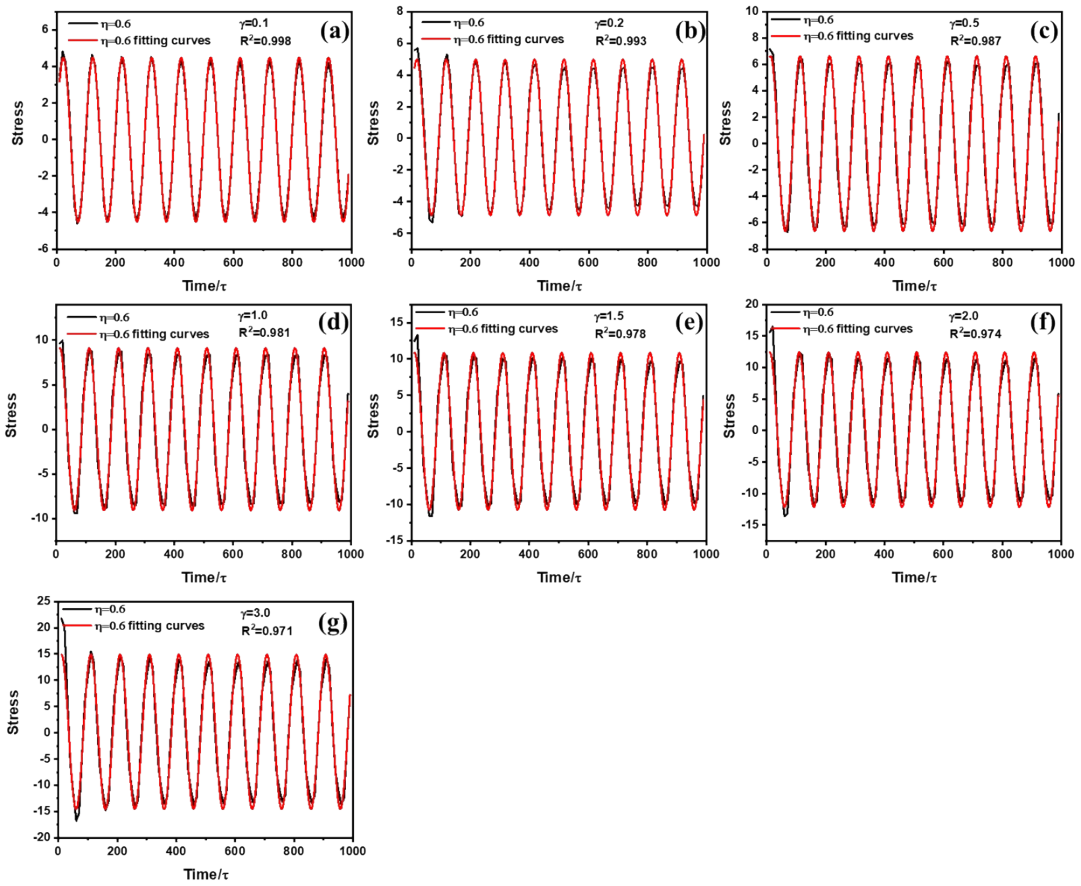
$\eta=0.2$



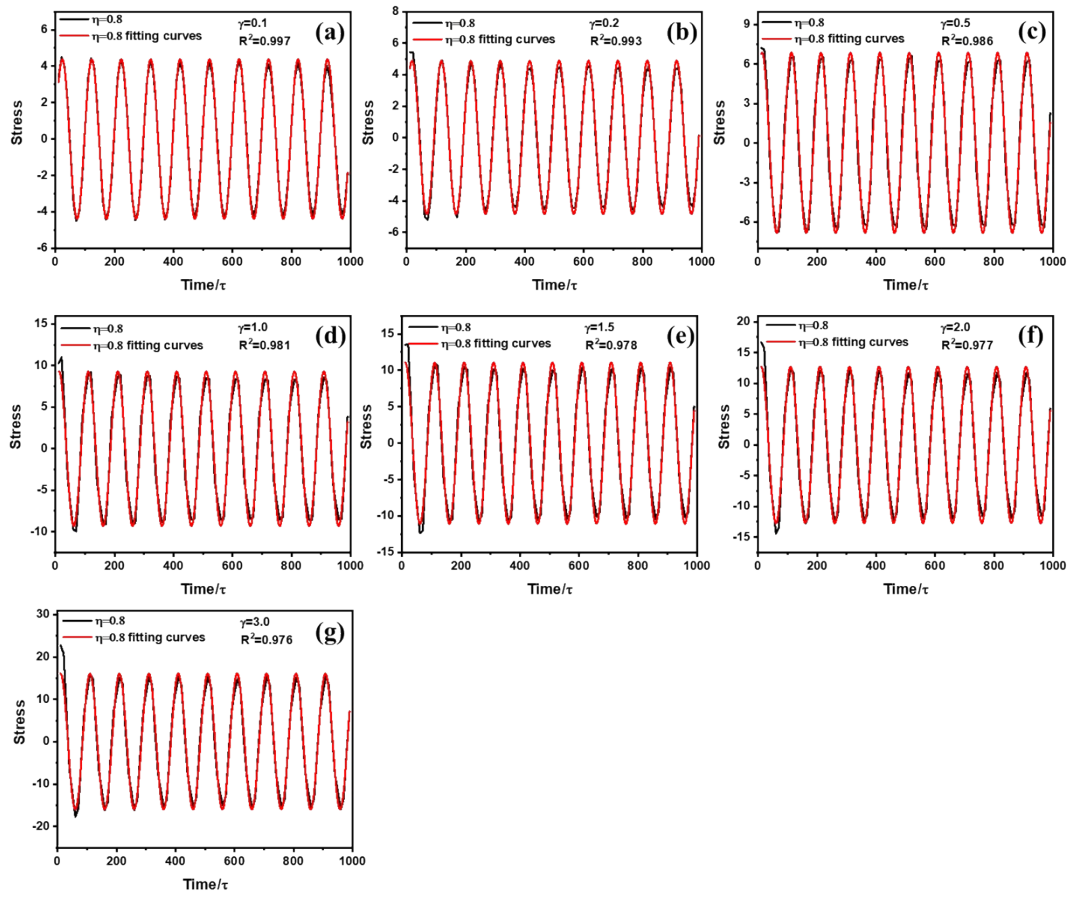
$\eta=0.4$



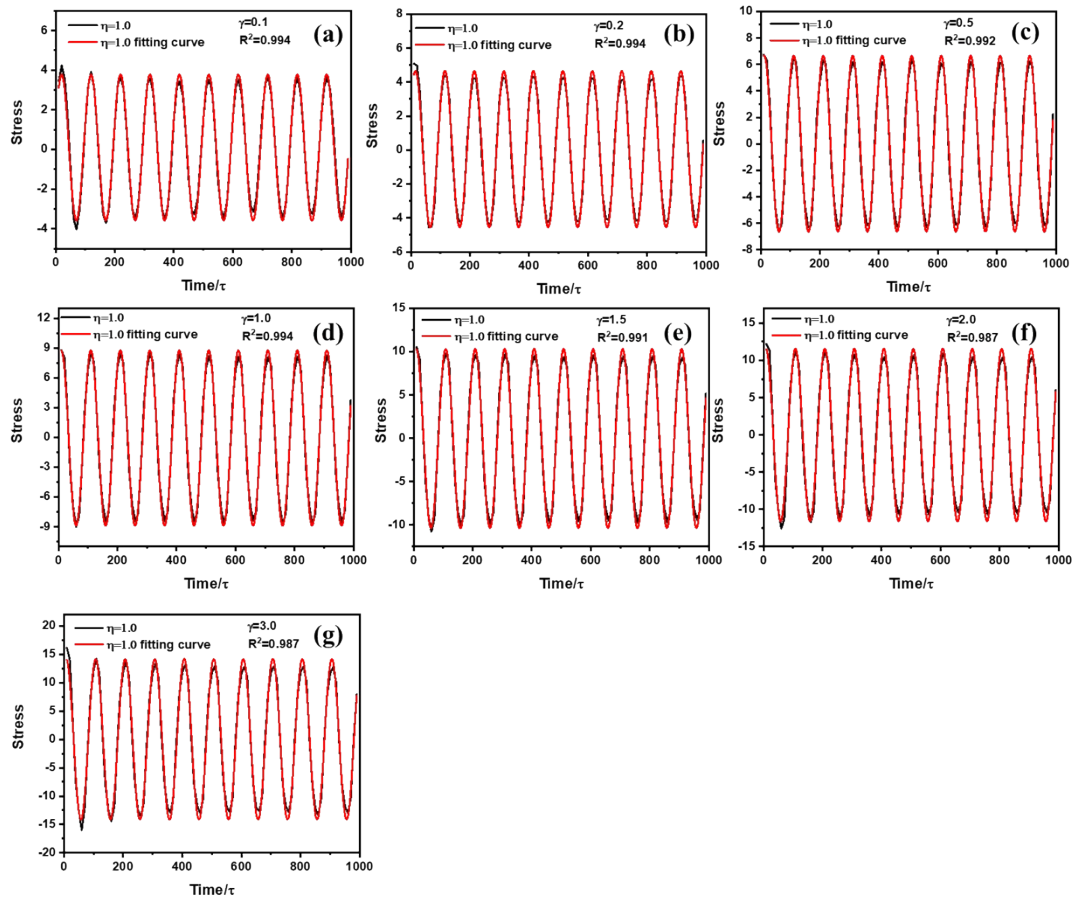
$\eta=0.6$



$\eta=0.8$



$\eta=1.0$



$\eta_s=1.0$

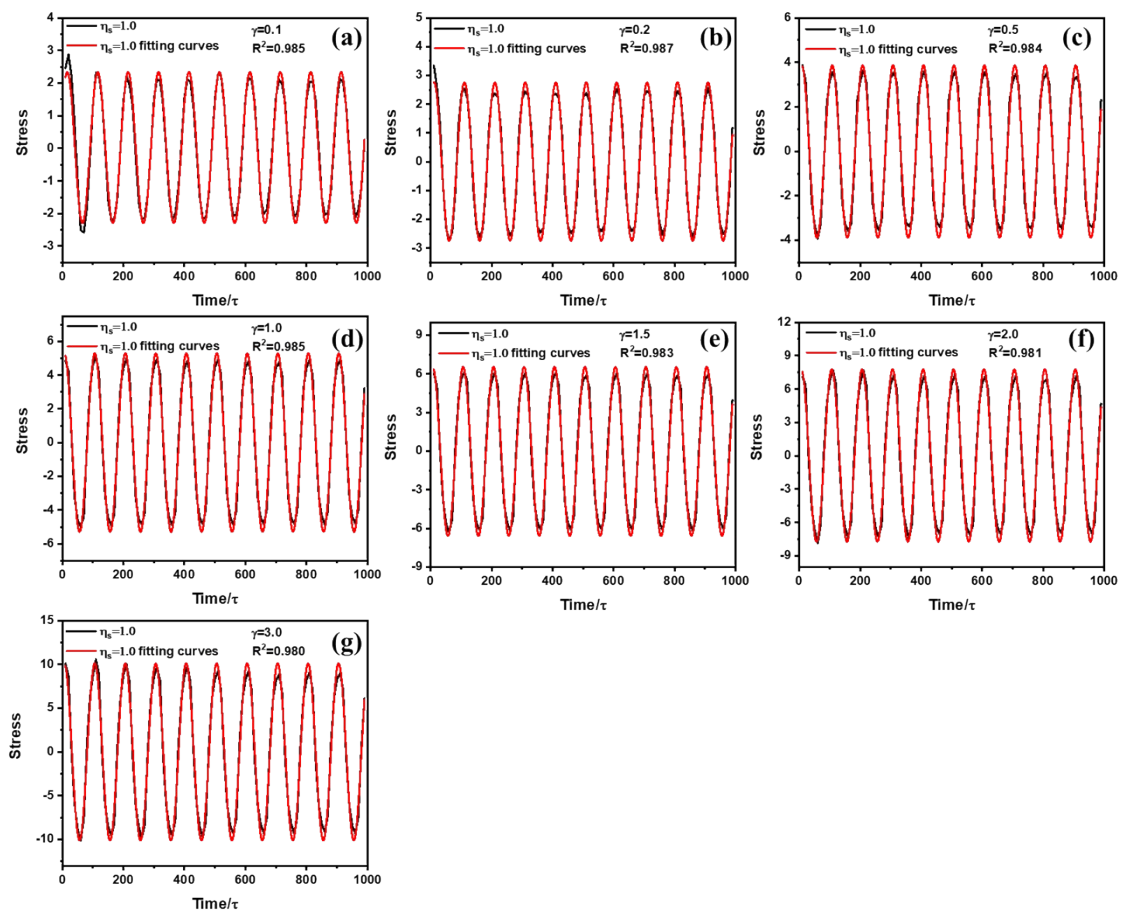


Figure S5. Shear stress-strain curves of SSPNs with different η , where (a) $\gamma=0.1$; (b) $\gamma=0.2$; (c) $\gamma=0.5$; (d) $\gamma=1.0$; (e) $\gamma=1.5$; (f) $\gamma=2.0$; (g) $\gamma=3.0$;

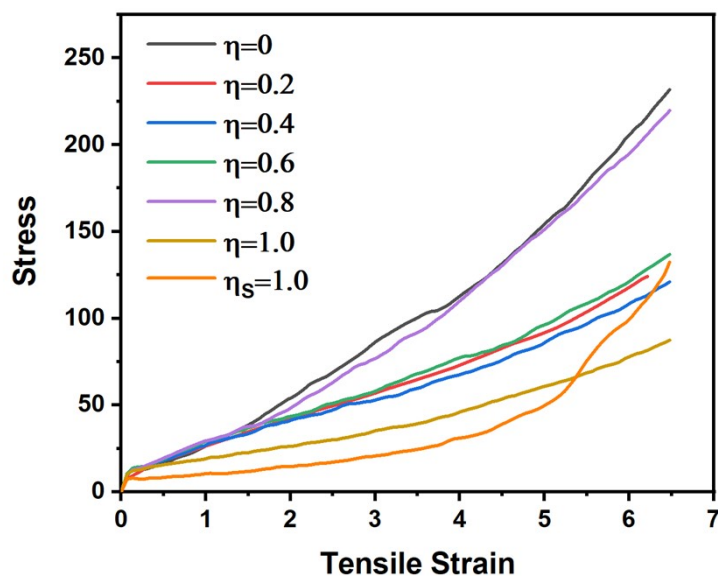


Figure S6. The stress-strain curve for different η .

Table S2. R_g of various L . Noted that $\eta = 0.8$

L (σ)	R_g (σ)
5	3.66
10	4.79
15	8.85
20	9.07

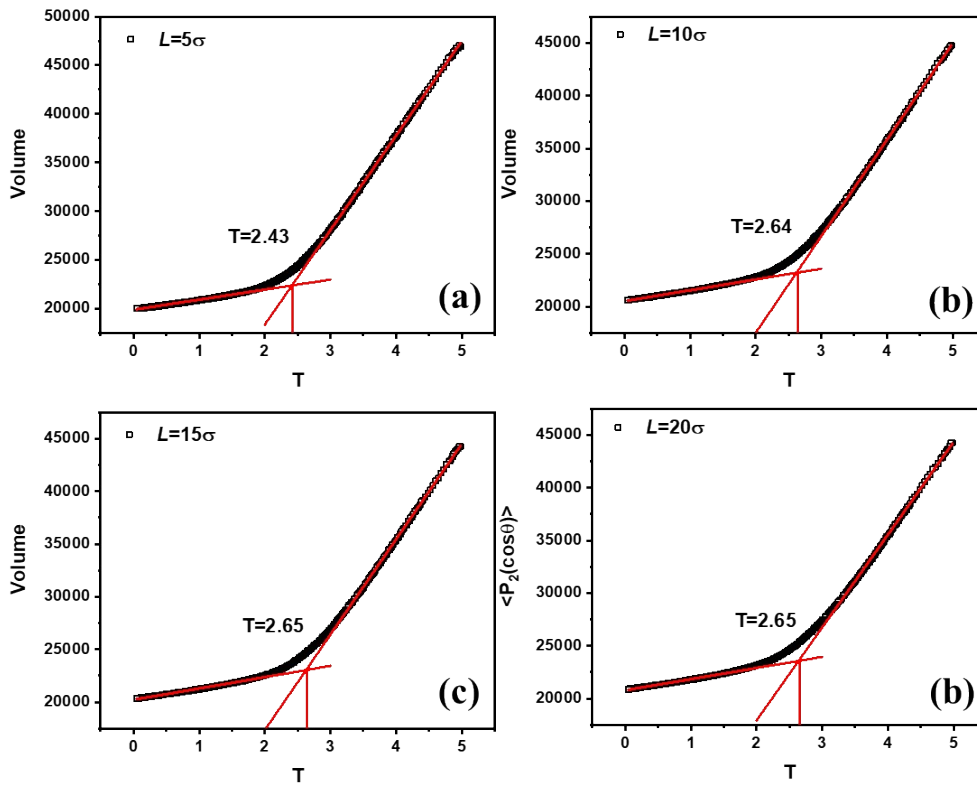


Figure S7. The glass transition temperature for PNCs when : (a) $L = 5\sigma$; (b) $L = 10\sigma$; (c) $L = 15\sigma$; (d) $L = 20\sigma$. Noted that $\eta = 0.8$.

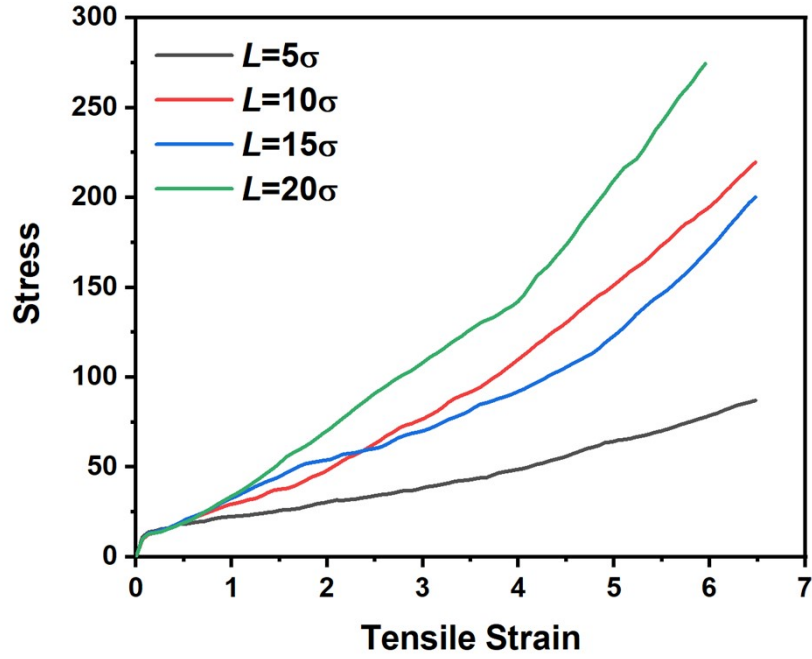
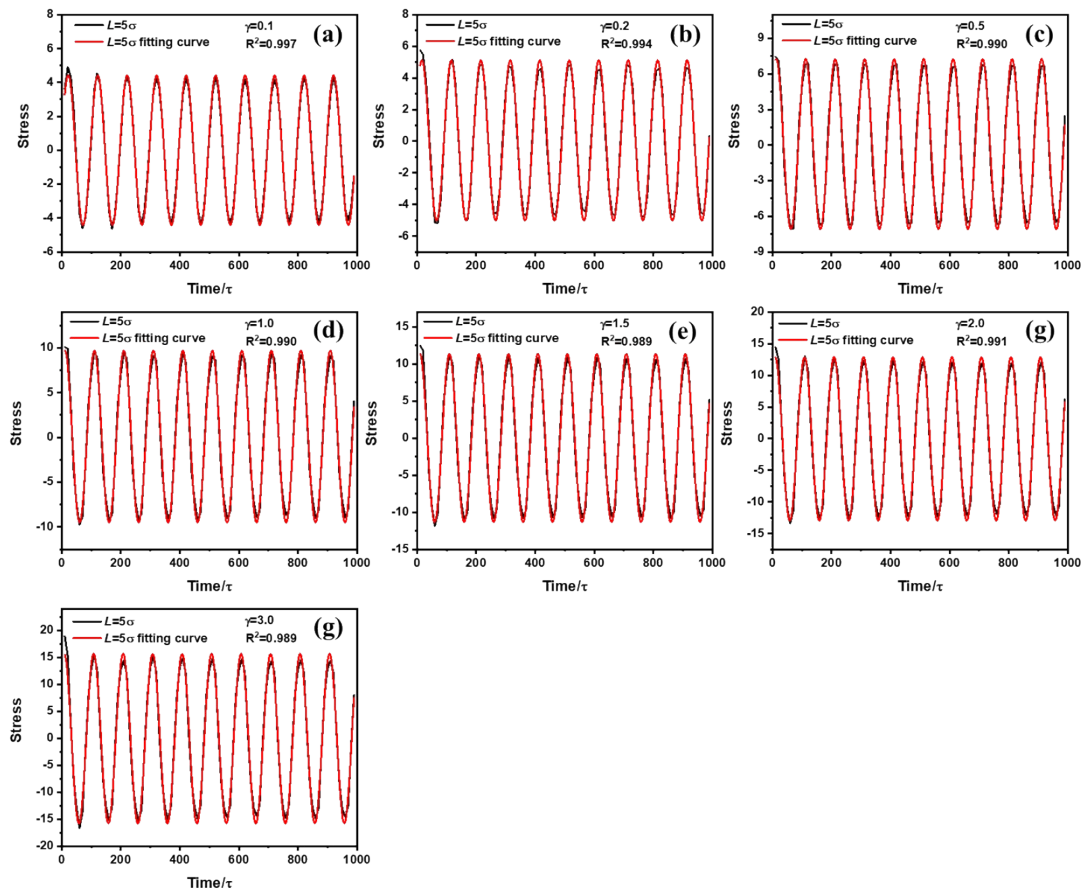
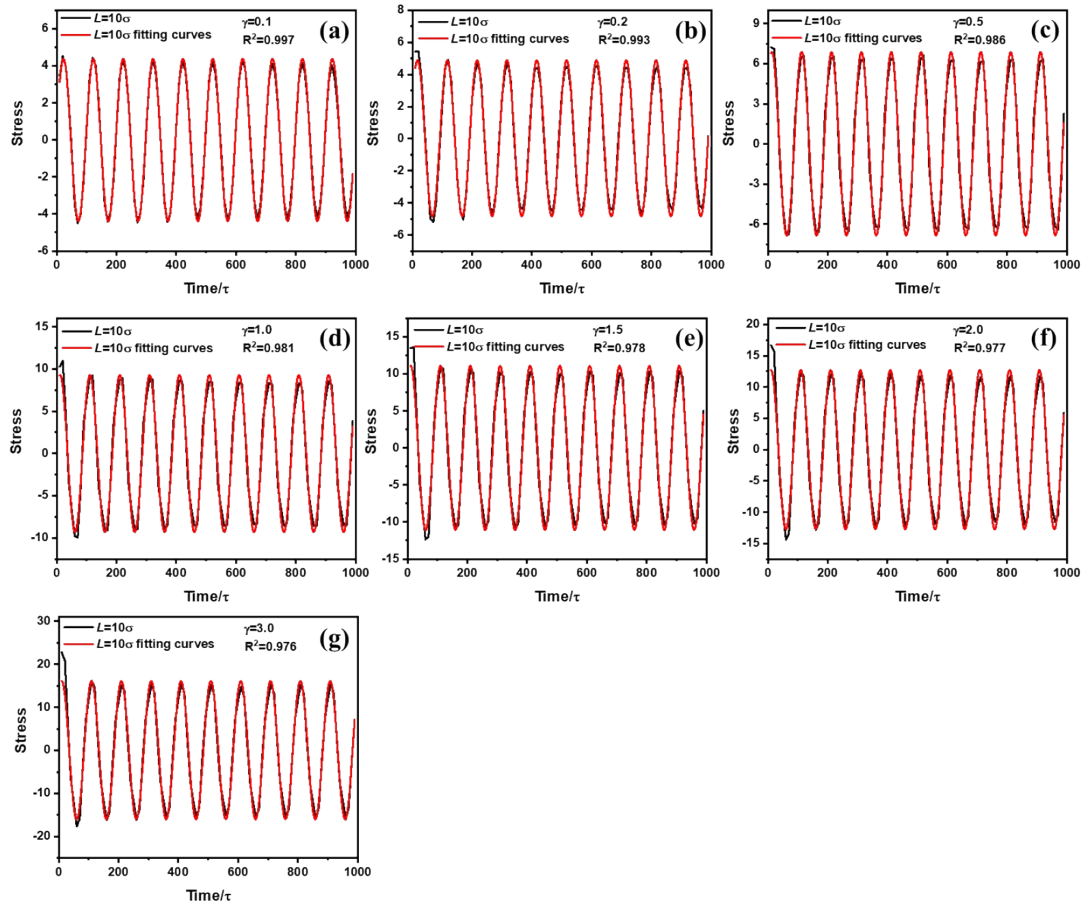


Figure S8. The stress-strain curve for different η .

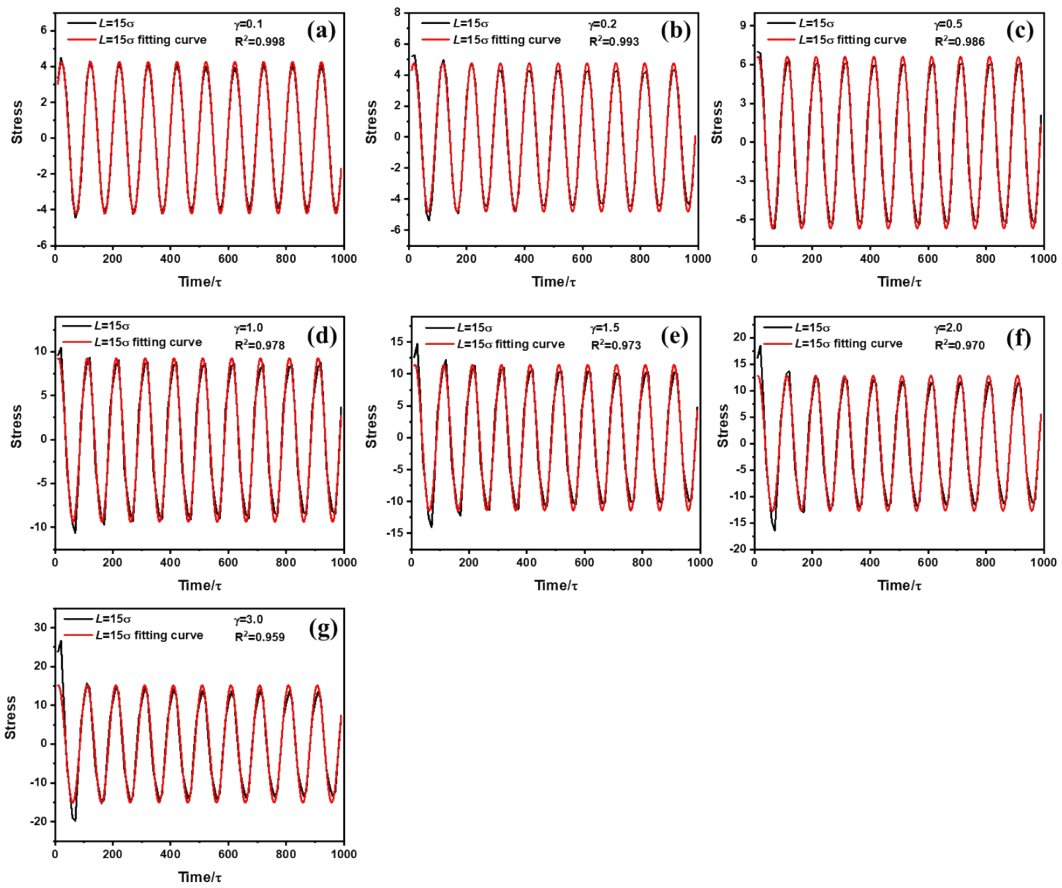
$L = 5\sigma$



$L = 10\sigma$



$L = 15\sigma$



$$L = 20\sigma$$

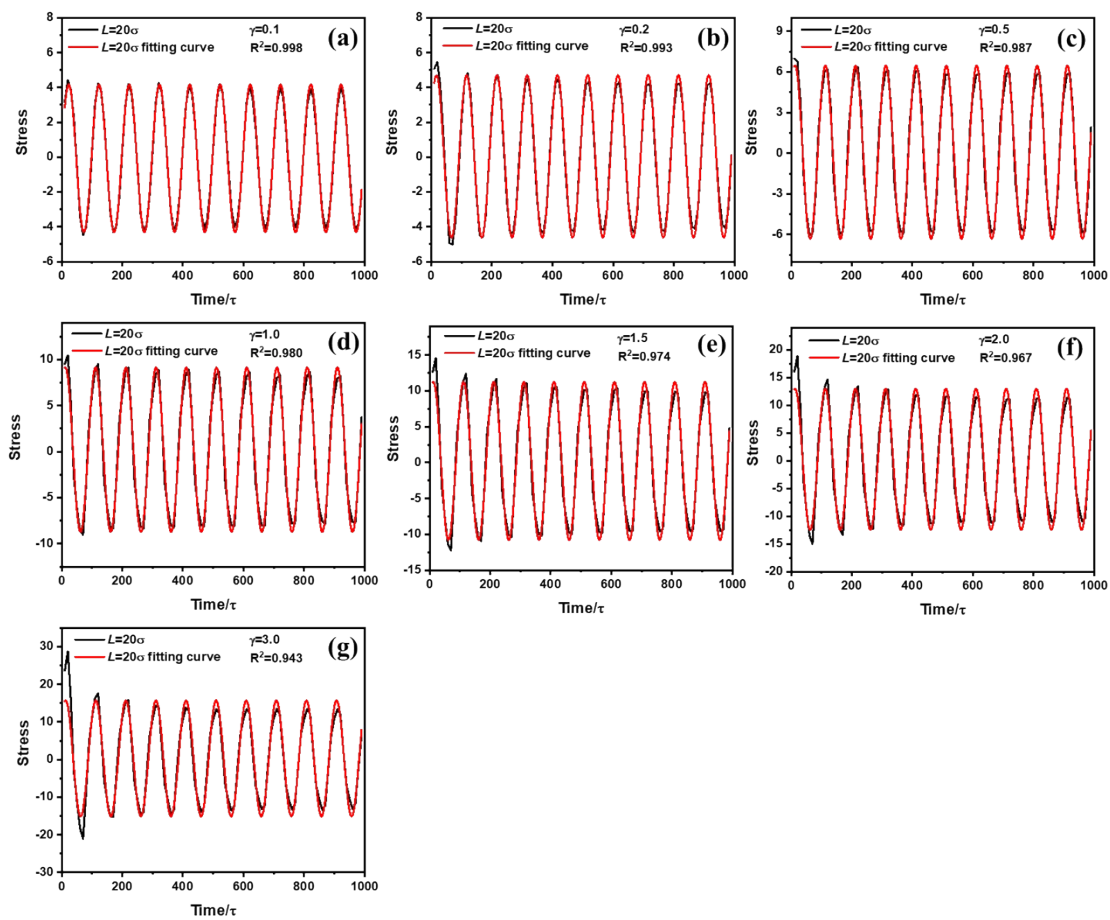


Figure S9. Shear stress-strain curves of SSPNs with different L , where (a) $\gamma=0.1$; (b) $\gamma=0.2$; (c) $\gamma=0.5$; (d) $\gamma=1.0$; (e) $\gamma=1.5$; (f) $\gamma=2.0$; (g) $\gamma=3.0$;